An Enhanced Predictive Location Tracking Scheme with Deficient Signal Sources for Wireless Networks

Po-Hsuan Tseng and Kai-Ten Feng
Department of Electrical Engineering
National Chiao Tung University
Hsinchu, Taiwan
walker.cm90@nctu.edu.tw and ktfeng@mail.nctu.edu.tw

***Abstract*—Location estimation and tracking for the mobile devices have attracted a significant amount of attention in recent years. The location estimators associated with the Kalman filtering techniques are exploited to both acquire location estimation and trajectory tracking for the mobile devices. However, most of the existing schemes become inapplicable for location tracking due to the deficiency of signal sources. In this paper, the enhanced predictive location tracking (EPLT) are proposed to alleviate this problem. The EPLT scheme utilizes the predictive information obtained from the Kalman filter in order to provide the additional signal inputs for the location estimator. Furthermore, the EPLT scheme incorporates the geometric dilution of precision (GDOP) information into the algorithm design. Persistent accuracy for location tracking can be achieved by adopting the proposed EPLT scheme, especially with inadequate signal sources. Numerical results demonstrate that the EPLT algorithm can achieve better precision in comparison with other location tracking schemes.**

I. Introduction

Wireless location technologies, which are designated to estimate the position of a mobile station (MS), have drawn a lot of attention over the past few decades. With the assistance of the information derived from the positioning system, the required performance and objectives for the targeting MS can be achieved with augmented robustness. In recent years, there are increasing demands for commercial applications to adopt the location information within their system design, such as the navigation systems, the health care systems and the wireless sensor networks. With the emergent interests in the location-based services, the location estimation and tracking algorithms with enhanced precision become necessitate for the applications under different circumstances.

The network-based location estimation schemes have been widely proposed and employed in the wireless communication system. These schemes locate the position of a MS based on the measured radio signals from its neighborhood base stations (BSs). In addition to the estimation of a MS's position, trajectory tracking of a moving MS has been studied [1], [2] to enhance the accuracy of location estimation. The Kalman tracking (KT) scheme [1] distinguishes the linear part from the originally nonlinear equations for location estimation. The linear aspect is exploited within the Kalman filtering formulation; while the nonlinear term is served as an external measurement input to the Kalman filter. The cascade location tracking (CLT) scheme as proposed in [2] utilizes the two-step least square (LS) method for initial location estimation of the MS and the cascaded Kalman filtering technique to trace the position of the MS based on its previously estimated data. However, the wireless location tracking problem with insufficient signal sources has not been addressed in previous studies. In the cellular-based networks, three BSs are required in order to provide three signal sources for the time-of-arrival (TOA) based location estimation. Nevertheless, the scenario with sufficient signal sources does not always happen in real circumstances, e.g. under rural environments or city valley with blocking buildings. In real-time tracking case, the situation of temporary blackouts of signal would be encountered with a high probability due to MS's mobility. It will be beneficial to provide consistent accuracy for location tracking under various environments.

It is noted that the design of the predictive location tracking (PLT) scheme was presented in our previous work in [3]. The PLT algorithm is proposed to improve the problem by utilizing the predictive information obtained from the Kalman filter with insufficient measurement inputs, i.e., with only two BSs or a single BS available to be exploited. In this paper, an enhanced predictive location tracking (EPLT) scheme is proposed by adopting the geometric dilution of precision (GDOP) concept into its formulation in order to further enhance the performance of the original PLT algorithm. The position of the virtual signal source is relocated for the purpose of achieving the minimum GDOP value with respect to the MS's position. In general, location estimation under higher standard deviations may yield degraded performance. It will be evaluated in the simulation that EPLT can still provide consistent precision with different noise model for location tracking comparing to the PLT scheme.

The remainder of this paper is organized as follows. Section II briefly describes the modeling of the signal sources and the GDOP metric. The architecture overview and formulation of the proposed EPLT scheme are explained in Section III.

[1]This work was in part funded by the Aiming for the Top University and Elite Research Center Development Plan, NSC 96-2221-E-009-016, the MediaTek research center at National Chiao Tung University, and the Universal Scientific Industrial (USI) Co., Taiwan.

Section IV illustrates the performance evaluation of the proposed EPLT scheme in comparison with the existing location tracking techniques. Section V draws the conclusions.

II. Preliminaries

A. Mathematical Modeling

In order to facilitate the design of the proposed EPLT algorithm, the signal model for the TOA measurements is utilized. The set $\boldsymbol{r}_k$ contains all the available measured relative distance at the k^{th} time step, i.e., $\boldsymbol{r}_k = \{r_{1,k}, \ldots, r_{i,k}, \ldots, r_{N_k,k}\}$, where N_k denotes the number of available BSs at the time step k. The measured relative distance between the MS and the i^{th} BS obtained at the k^{th} time step can be represented as

$$r_{i,k} = c \cdot t_{i,k} = \zeta_{i,k} + n_{i,k} + e_{i,k} \quad i = 1, 2, ..., N_k \tag{1}$$

where $t_{i,k}$ denotes the TOA measurement obtained from the i^{th} BS at the k^{th} time step, and c is the speed of light. $r_{i,k}$ is contaminated with the TOA measurement noise $n_{i,k}$ and the NLOS error $e_{i,k}$. It is noted that the measurement noise $n_{i,k}$ is in general considered as zero mean with Gaussian distribution. On the other hand, the NLOS error $e_{i,k}$ is modeled as exponentially-distributed for representing the positive bias due to the NLOS effect [4]. The noiseless relative distance $\zeta_{i,k}$ (in (1)) between the MS's true position and the i^{th} BS can be obtained as

$$\zeta_{i,k} = [(x_k - x_{i,k})^2 + (y_k - y_{i,k})^2]^{\frac{1}{2}} \tag{2}$$

where $\boldsymbol{x}_k = [x_k \; y_k]$ represents the MS's true position and $\boldsymbol{x}_{i,k} = [x_{i,k} \; y_{i,k}]$ is the location of the i^{th} BS for $i = 1$ to N_k. Therefore, the set of all the available BSs at the k^{th} time step can be obtained as $\boldsymbol{P}_{BS,k} = \{\boldsymbol{x}_{1,k}, \ldots, \boldsymbol{x}_{i,k}, \ldots, \boldsymbol{x}_{N_k,k}\}$.

B. Geometric Dilution of Precision (GDOP)

The GDOP [5] associated with the position error is utilized as an index for observing the location precision of the MS under different geometric location within the networks, e.g. the cellular or the satellite networks. In general, a larger GDOP value corresponds to a comparably worse geometric layout (established by the MS and its associated BSs), which consequently results in augmented errors for location estimation. Considering the MS's location under the two-dimensional coordinate, the GDOP value (G) obtained at the position $\boldsymbol{x}_k$ can be represented as

$$\mathrm{G}_{\boldsymbol{x}_k} = \left\{\text{trace}\left[(\mathbf{H}_{\boldsymbol{x}_k}^T \mathbf{H}_{\boldsymbol{x}_k})^{-1}\right]\right\}^{\frac{1}{2}} \tag{3}$$

where

$$\mathbf{H}_{\boldsymbol{x}_k} = \begin{bmatrix} \frac{x_k - x_{1,k}}{\zeta_{1,k}} & \frac{y_k - y_{1,k}}{\zeta_{1,k}} \\ \cdots & \cdots \\ \frac{x_k - x_{i,k}}{\zeta_{i,k}} & \frac{y_k - y_{i,k}}{\zeta_{i,k}} \\ \cdots & \cdots \\ \frac{x_k - x_{N_k,k}}{\zeta_{N_k,k}} & \frac{y_k - y_{N_k,k}}{\zeta_{N_k,k}} \end{bmatrix} \tag{4}$$

It is noted that the elements within the matrix $\mathbf{H}_{\boldsymbol{x}_k}$ can be acquired from (2).

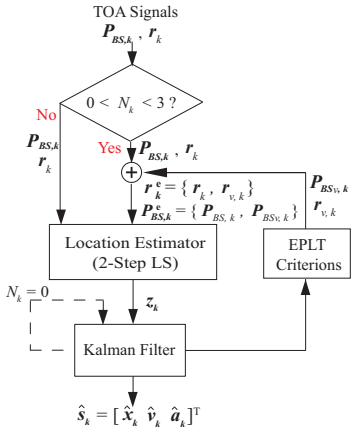

Fig. 1. The architecture diagrams of the proposed EPLT scheme

III. Proposed EPLT Algorithm

A. Architecture Overview

The objective of the proposed EPLT algorithm is to utilize the predictive information acquired from the Kalman filter to serve as the assisted measurement inputs while the environments are deficient with signal sources. Fig. 1 illustrates the system architectures of the proposed EPLT scheme. The TOA signals ($\boldsymbol{r}_k$ as in (1)) associated with the corresponding location set of the BSs ($\boldsymbol{P}_{BS,k}$) are obtained as the signal inputs to each of the system, which result in the estimated state vector of the MS, i.e., $\hat{\boldsymbol{s}}_k = [\hat{\boldsymbol{x}}_k \; \hat{\boldsymbol{v}}_k \; \hat{\boldsymbol{a}}_k]^T$ where $\hat{\boldsymbol{x}}_k = [\hat{x}_k \; \hat{y}_k]$ represents the MS's estimated position, $\hat{\boldsymbol{v}}_k = [\hat{v}_{x,k} \; \hat{v}_{y,k}]$ is the estimated velocity, and $\hat{\boldsymbol{a}}_k = [\hat{a}_{x,k} \; \hat{a}_{y,k}]$ denotes the estimated acceleration.

It is noticed that the EPLT algorithm adopts the architecture of the CLT scheme, i.e., the two-step LS method cascaded with the Kalman filter. The EPLT algorithm will be the same as the CLT scheme while the number of available BSs is greater than or equal to three, i.e., $N_k \geq 3$. It is also noted that the EPLT scheme will perform the same as the CLT method under the case with no signal input, i.e., $N_k = 0$. However, the effectiveness of the EPLT scheme is revealed as $1 \leq N_k < 3$, i.e., with deficient measurement inputs. The predictive state information obtained from the Kalman filter is utilized for acquiring the assisted information, which will be fed back into the location estimator. The extended sets for the locations of the BSs (i.e., $\boldsymbol{P}_{BS,k}^e = \{\boldsymbol{P}_{BS,k}, \boldsymbol{P}_{BS_v,k}\}$) and the measured relative distances (i.e., $\boldsymbol{r}_k^e = \{\boldsymbol{r}_k, \boldsymbol{r}_{v,k}\}$) will be utilized as the inputs to the location estimator. The sets of the virtual BS's locations $\boldsymbol{P}_{BS_v,k}$ and the virtual measurements $\boldsymbol{r}_{v,k}$ are defined as follows.

Definition 1 (Virtual Base Stations). *The virtual Base Stations are considered as the designed locations for assisting the location tracking of the MS under the environments with deficient signal sources. The set of virtual BSs $\boldsymbol{P}_{BS_v,k}$ is defined under two different numbers of N_k as*

$$\boldsymbol{P}_{BS_v,k} = \begin{cases} \{\boldsymbol{x}_{v_1,k}\} & \text{for } N_k = 2 \\ \{\boldsymbol{x}_{v_1,k}, \boldsymbol{x}_{v_2,k}\} & \text{for } N_k = 1 \end{cases} \tag{5}$$

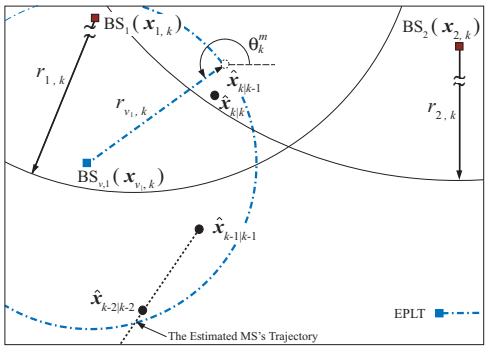

Fig. 2. The schematic diagram of the two-BSs case for the proposed EPLT scheme

Definition 2 (Virtual Measurements). *The virtual measurements are utilized to provide assisted measurement inputs while the signal sources are insufficient. Associating with the designed set of virtual BSs $\boldsymbol{P}_{BS_v,k}$, the corresponding set of virtual measurements $\boldsymbol{r}_{v,k}$ is defined as*

$$\boldsymbol{r}_{v,k} = \begin{cases} \{r_{v_1,k}\} & \text{for } N_k = 2 \\ \{r_{v_1,k},\, r_{v_2,k}\} & \text{for } N_k = 1 \end{cases} \tag{6}$$

It is noticed that the major tasks of EPLT scheme are to design and to acquire the values of $\boldsymbol{P}_{BS_v,k}$ and $\boldsymbol{r}_{v,k}$ for the two cases (i.e., N_k = 1 and 2) with inadequate signal sources. In traditional location tracking schemes such as the KT and the CLT schemes, the estimated state vector $\hat{\boldsymbol{s}}_k$ can only be updated by the internal prediction mechanism of the Kalman filter while there are insufficient numbers of BSs. The location estimator (i.e., the two-step LS method) is consequently disabled owing to the inadequate number of the signal sources. The tracking capabilities of both schemes significantly depend on the correctness of the Kalman filter's prediction mechanism. Therefore, the performance for location tracking can be severely degraded due to the changing behavior of the MS, i.e., with the variations from the MS's acceleration. The proposed EPLT algorithm can still provide satisfactory tracking performance with deficient measurement inputs. Comparing to the PLT scheme which is presented in our previous work, the EPLT algorithm has the same set of virtual measurement $\boldsymbol{r}_{v,k}$ and enhances the precision and the robustness of the location estimation from the PLT scheme by considering the GDOP effect with different virtual BSs set $\boldsymbol{P}_{BS_v,k}$.

B. Formulation of EPLT Algorithm

The proposed EPLT scheme will be explained in this section. As shown in Fig. 1, the measurement and state equations for the Kalman filter can be represented as

$$\boldsymbol{z}_k = \mathbf{M}\hat{\boldsymbol{s}}_k + \boldsymbol{m}_k \tag{7}$$

$$\hat{\boldsymbol{s}}_k = \mathbf{F}\hat{\boldsymbol{s}}_{k-1} + \boldsymbol{p}_k \tag{8}$$

where $\hat{\boldsymbol{s}}_k = [\hat{\boldsymbol{x}}_k \;\; \hat{\boldsymbol{v}}_k \;\; \hat{\boldsymbol{a}}_k]^T$. The variables $\boldsymbol{m}_k$ and $\boldsymbol{p}_k$ denote the measurement and the process noises associated with the covariance matrices $\mathbf{R}$ and $\mathbf{Q}$ within the Kalman filtering formulation. The measurement vector $\boldsymbol{z}_k = [\hat{x}_{ls,k} \;\; \hat{y}_{ls,k}]^T$ represents the measurement input which is obtained from the output of the two-step LS estimator at the k^{th} time step (as in Fig. 1.(c)). The matrix $\mathbf{M}$ and the state transition matrix $\mathbf{F}$ can be obtained as

$$\mathbf{M} = \begin{bmatrix} 1 & 0 & 0 & 0 & 0 & 0 \\ 0 & 1 & 0 & 0 & 0 & 0 \end{bmatrix} \tag{9}$$

$$\mathbf{F} = \begin{bmatrix} 1 & 0 & \Delta t & 0 & \frac{1}{2}\Delta t^2 & 0 \\ 0 & 1 & 0 & \Delta t & 0 & \frac{1}{2}\Delta t^2 \\ 0 & 0 & 1 & 0 & \Delta t & 0 \\ 0 & 0 & 0 & 1 & 0 & \Delta t \\ 0 & 0 & 0 & 0 & 1 & 0 \\ 0 & 0 & 0 & 0 & 0 & 1 \end{bmatrix} \tag{10}$$

where Δt denotes the sample time interval. Two cases (i.e., the two-BSs case and the single-BS case) are considered as follows:

1) Two-BSs Case: As shown in Fig. 2, it is assumed that only two BSs (i.e., BS_1 and BS_2) associated with two TOA measurements are available at the time step k in consideration. The main target is to introduce an additional virtual BS along with its virtual measurement (i.e., $\boldsymbol{P}_{BS_v,k} = \{\boldsymbol{x}_{v_1,k}\}$ and $\boldsymbol{r}_{v,k} = \{r_{v_1,k}\}$) by acquiring the predictive output information from the Kalman filter. Knowing that there are predicting and correcting phases within the Kalman filtering formulation, the predictive state can therefore be utilized to compute the supplementary virtual measurement $r_{v_1,k}$ as

$$r_{v_1,k} = \|\hat{\boldsymbol{x}}_{k|k-1} - \hat{\boldsymbol{x}}_{k-1|k-1}\| \tag{11}$$

where $\hat{\boldsymbol{x}}_{k|k-1}$ denotes the predicted MS's position at time step k; while $\hat{\boldsymbol{x}}_{k-1|k-1}$ is the corrected MS's position obtained at the $(k-1)^{th}$ time step. It is noticed that both values are available at the $(k-1)^{th}$ time step. The virtual measurement $r_{v_1,k}$ is defined as the distance between the previous location estimate ($\hat{\boldsymbol{x}}_{k-1|k-1}$) and the predicted MS's position ($\hat{\boldsymbol{x}}_{k|k-1}$) as the possible position of the MS.

The objective of the EPLT scheme is to acquire the angle θ_k of $\boldsymbol{x}_{v_1,k}$ such that the predicted MS ($\hat{\boldsymbol{x}}_{k|k-1}$) will possess a minimal GDOP value within its network topology for location estimation. As illustrated in Fig. 2, the following equality can be obtained based on the geometric relationship:

$$\hat{\boldsymbol{x}}_{k|k-1} - \boldsymbol{x}_{v_1,k} = (-r_{v_1,k} \cdot \cos\theta_k,\; -r_{v_1,k} \cdot \sin\theta_k) \tag{12}$$

It is noticed that the angle θ_k is rotated from the positive x-axis based on the predicted MS ($\hat{\boldsymbol{x}}_{k|k-1}$). As mentioned above, the position of the virtual BS ($\boldsymbol{x}_{v_1,k}$) is designed such that the predicted MS ($\hat{\boldsymbol{x}}_{k|k-1}$) will be located at a minimal GDOP position based on the extended geometric set $\boldsymbol{P}^{e}_{BS,k}$ = $\{\boldsymbol{x}_{1,k}, \boldsymbol{x}_{2,k}, \boldsymbol{x}_{v_1,k}\}$. By incorporating (12) into (3) and (4), the GDOP value (i.e., $G_{\hat{\boldsymbol{x}}_{k|k-1}}$) computed at the predicted MS's position $\hat{\boldsymbol{x}}_{k|k-1} = (\hat{x}_{k|k-1}, \hat{y}_{k|k-1})$ can be obtained. The associated matrix $\mathbf{H}_{\hat{\boldsymbol{x}}_{k|k-1}}$ becomes

$$\mathbf{H}_{\hat{\boldsymbol{x}}_{k|k-1}} = \begin{bmatrix} \frac{\hat{x}_{k|k-1}-x_{1,k}}{r_{1,k}} & \frac{\hat{y}_{k|k-1}-y_{1,k}}{r_{1,k}} \\ \frac{\hat{x}_{k|k-1}-x_{2,k}}{r_{2,k}} & \frac{\hat{y}_{k|k-1}-y_{2,k}}{r_{2,k}} \\ -\cos\theta_k & -\sin\theta_k \end{bmatrix} \tag{13}$$

It is noted that the noiseless relative distances $\zeta_{i,k}$ in (3)

$$\Gamma = \frac{2[r_{2,k}^2(\hat{x}_{k|k-1}-x_{1,k})(\hat{y}_{k|k-1}-y_{1,k})+r_{1,k}^2(\hat{x}_{k|k-1}-x_{2,k})(\hat{y}_{k|k-1}-y_{2,k})]}{r_{2,k}^2(\hat{x}_{k|k-1}-x_{1,k})^2-r_{2,k}^2(\hat{y}_{k|k-1}-y_{1,k})^2+r_{1,k}^2(\hat{x}_{k|k-1}-x_{2,k})^2-r_{1,k}^2(\hat{y}_{k|k-1}-y_{2,k})^2} \tag{14}$$

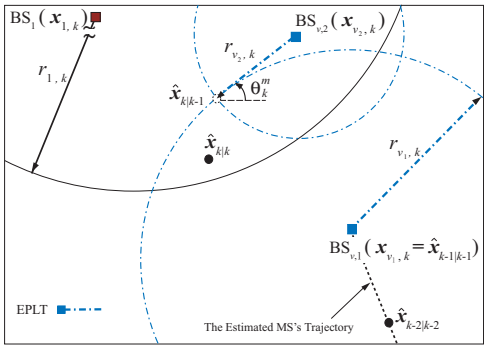

Fig. 3. The schematic diagram of the single-BS case for the proposed EPLT scheme

are approximately replaced by $r_{i,k}$ in (13) since $\zeta_{i,k}$ are considered unattainable. It can be observed from (13) that the matrix $\mathbf{H}_{\hat{\boldsymbol{x}}_{k|k-1}}$ associated with the resulting $\mathrm{G}_{\hat{\boldsymbol{x}}_{k|k-1}}$ value are regarded as functions of the angle θ_k, i.e., $\mathbf{H}_{\hat{\boldsymbol{x}}_{k|k-1}}(\theta_k)$ and $\mathrm{G}_{\hat{\boldsymbol{x}}_{k|k-1}}(\theta_k)$. Based on the objective of the EPLT scheme, the angle θ_k^m which results in the minimal GDOP value can therefore be acquired as

$$\theta_k^m = \arg\left\{\min_{\forall\theta_k} \mathrm{G}_{\hat{\boldsymbol{x}}_{k|k-1}}(\theta_k)\right\} \tag{15}$$

It is intuitive to observed that (15) can be achieved if the following conditions on the first and second derivatives of $\mathrm{G}_{\hat{\boldsymbol{x}}_{k|k-1}}(\theta_k)$ are satisfied:

$$\left[\frac{\partial \mathrm{G}_{\hat{\boldsymbol{x}}_{k|k-1}}(\theta_k)}{\partial\theta_k}\right]_{\theta_k=\theta_k^m} = 0 \tag{16}$$

$$\left[\frac{\partial^2 \mathrm{G}_{\hat{\boldsymbol{x}}_{k|k-1}}(\theta_k)}{\partial^2\theta_k}\right]_{\theta_k=\theta_k^m} > 0 \tag{17}$$

By substituting (13) and (3) into (16), the angle θ_k^m can be computed as

$$\theta_k^m = \tan^{-1}\left(\frac{1\pm\sqrt{1+\Gamma^2}}{\Gamma}\right) \tag{18}$$

where Γ is as in (14) at the top of the page. It is noted that the selection for either the positive or the negative value of θ_k^m is determined by (17). At each time instant k, the relative angle θ_k^m between $\hat{\boldsymbol{x}}_{k|k-1}$ and $\boldsymbol{x}_{v_1,k}$ can therefore be obtained such that $\hat{\boldsymbol{x}}_{k|k-1}$ is located at the position with a minimal GDOP value based on its current network layout.

2) Single-BS Case: In this case, only one BS (i.e., BS_1) with one TOA measurement input is available at the k^{th} time step (as shown in Fig. 3). Two additional virtual BSs and measurements are required for the computation of the two-step LS estimator, i.e., $\boldsymbol{P}_{BS_v,k} = \{\boldsymbol{x}_{v_1,k}, \boldsymbol{x}_{v_2,k}\}$ and $\boldsymbol{r}_{v,k} = \{r_{v_1,k}, r_{v_2,k}\}$. Similar to the previous case, the first virtual measurement $r_{v_1,k}$ is acquired as in (11) by considering the distance between previous estimated MS position $\hat{\boldsymbol{x}}_{k-1|k-1}$ and the predicted MS's position $\hat{\boldsymbol{x}}_{k|k-1}$. On the other hand, the second virtual measurement $r_{v_2,k}$ is defined as the average prediction error obtained from the Kalman filtering formulation by accumulating the previous time steps as

$$r_{v_2,k} = \frac{1}{k-1}\sum_{i=1}^{k-1}\|\hat{\boldsymbol{x}}_{i|i} - \hat{\boldsymbol{x}}_{i|i-1}\| \tag{19}$$

It is noted that $r_{v_2,k}$ is obtained as the mean prediction error until the $(k-1)^{th}$ time step. In the case while the Kalman filter is capable of providing sufficient accuracy in its prediction phase, the virtual measurement $r_{v_2,k}$ may approach zero value. Associating with the single measurement $r_{1,k}$ from BS_1, the two additional virtual measurements $r_{v_1,k}$ and $r_{v_2,k}$ result in a constrained region (as in Fig. 3) for location estimation of the MS under the environments with insufficient signal sources.

In order to locate two virtual BSs by utilizing the equations as in (15) and (18), the first virtual BS is designed to be located at $\boldsymbol{x}_{v_1,k} = \hat{\boldsymbol{x}}_{k-1|k-1}$ associated with the first virtual measurement $r_{v_1,k}$ as defined in (11). The position of the second virtual BS ($\boldsymbol{x}_{v_2,k}$) is designed at a location with distance $r_{v_2,k}$ relative to the predicted MS's position $\hat{\boldsymbol{x}}_{k|k-1}$. Therefore, the following equations can be obtained based on the geometric relationships from Fig. 3:

$$\hat{\boldsymbol{x}}_{k|k-1} - \boldsymbol{x}_{v_2,k} = (-r_{v_2,k}\cdot\cos\theta_k^m,\ -r_{v_2,k}\cdot\sin\theta_k^m) \tag{20}$$

The relative angle θ_k^m between $\boldsymbol{x}_{v_2,k}$ and $\hat{\boldsymbol{x}}_{k|k-1}$ is determined by minimizing the GDOP value based on the predicted MS's position $\hat{\boldsymbol{x}}_{k|k-1}$. Both of the information from BS_1 and BS_{v_1} alone with the predicted MS's position $\hat{\boldsymbol{x}}_{k|k-1}$ are utilized for the computation of the angle θ_k^m (as in (15) and (18)). It is noticed that instead of altering the position of BS_{v_1}, the BS_{v_2}'s location is adjusted in order to acquire a better GDOP value for the predicted MS $\hat{\boldsymbol{x}}_{k|k-1}$. The design concept is primarily owing to the fact that the average prediction error is in general smaller than the length of each prediction within the Kalman filtering formulation, i.e., $r_{v_1,k} > r_{v_2,k}$. The expected MS's position $\hat{\boldsymbol{x}}_{k|k-1}$ is considered more sensitive to $r_{v_2,k}$ due to its smaller value comparing with $r_{1,k}$ and $r_{v_1,k}$. It will be beneficial to adjust the location of BS_{v_2} (by rotating the angle θ_k^m) such that a smaller GDOP value can be achieved at the predicted location of the MS ($\hat{\boldsymbol{x}}_{k|k-1}$). With the computation of the angle θ_k^m from the EPLT scheme, the collinear situation between BS_1 and BS_{v_2} can be avoided.

IV. Performance Evaluation

The model for the measurement noise of the TOA signals is selected as the Gaussian distribution with zero mean and 10 meters of standard deviation, i.e., $n_{i,k} \sim \mathcal{N}(0, 100)$. On the other hand, an exponential distribution $p_{e_{i,k}}(v)$ is assumed for

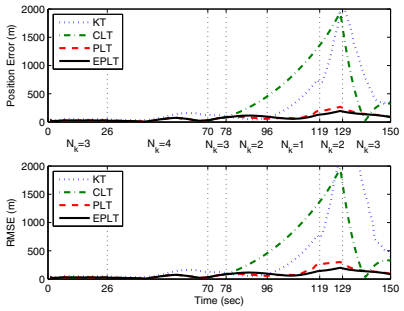

Fig. 4. Upper plot: the position error vs. the simulation time (sec); Lower plot: the RMSE vs. the simulation time (sec)

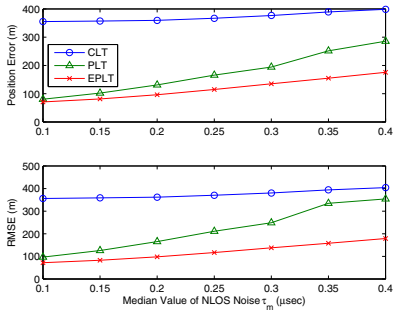

Fig. 5. Upper plot: the position error vs the median value of NLOS noise (τ_m); Lower plot: the RMSE vs the median value of NLOS noise (τ_m)

the NLOS noise model of the TOA measurements as

$$p_{e_{i,k}}(\upsilon) = \begin{cases} \frac{1}{\lambda_{i,k}} \exp\left(-\frac{\upsilon}{\lambda_{i,k}}\right) & \upsilon > 0 \\ 0 & \text{otherwise} \end{cases} \quad (21)$$

where $\lambda_{i,k} = c \cdot \tau_{i,k} = c \cdot \tau_m(\zeta_{i,k})^{\varepsilon}\rho$. The parameter $\tau_{i,k}$ is the RMS delay spread between the i^{th} BS to the MS. τ_m represents the median value of $\tau_{i,k}$, which is selected as 0.1 μs in the simulations. ε is the path loss exponent which is assumed to be 0.5. The shadow fading factor ρ is a log-normal random variable with zero mean and standard deviation σ_ρ chosen as 4 dB in the simulations. The parameters for the noise models as listed in this subsection primarily fulfill the environment while the MS is located within the rural area. It is noticed that the reason for selecting the rural area as the simulation scenario is due to its higher probability to suffer from deficiency of signal sources. Moreover, the sampling time Δt is chosen as 1 sec.

The performance comparisons between the KT scheme, the CLT scheme, the PLT scheme and the proposed EPLT algorithm are first conducted under the rural environment. The various numbers of BSs (i.e., the N_k values) that are available at different time intervals are illustrated in the middle of Fig. 4. For example, the number of available BSs is equal to three between the time interval (70,77). It can be seen that the number of BSs becomes insufficient (i.e., $N_k < 3$) from the time interval of t = 78 to 128 sec. The total simulation interval is set as 150 seconds. The acceleration is designed to vary at time t = 40, 55, 100, and 120 sec from $\boldsymbol{a}_k$ = ($a_{x,k}$, $a_{y,k}$) = (0.5, 0), (-1, 1.5), (0, 0), (0.5, 0), to (1, -2) m/sec^2. It is noted that the number of BSs becomes insufficient during the second acceleration change, i.e., at t = 78 sec. Fig. 4 illustrates the position error and the root mean square error (RMSE). It can be observed that the PLT and proposed EPLT algorithm outperform the conventional KT and CLT schemes. The main differences between these algorithms occur while the signal sources become insufficient within the time interval between t = 78 and 128 sec. The PLT and proposed EPLT schemes can still provide consistent location estimation and tracking. The major reason is attributed to the assisted information that is fed back into the location estimator while the signal sources are deficient.

In order to evaluate the sensitivity evaluation of the NLOS errors to the estimation performance, the position error and the RMSE as depicted in Fig. 5 are utilized to compare the three schemes under different NLOS errors, where the median value of the NLOS noises τ_m = 0.1, 0.3, and 0.4 corresponds to the rural, suburban, and urban environments. It is noted that both the estimation error and the RMSE are obtained as the average values acquired from the trajectory as designed in Fig. 4. Moreover, the performance obtained from the KT scheme is not illustrated in Fig. 5 due to its drastically degraded performance as the NLOS noises τ_m is increased. Owing to the consideration of the geometric layout, it can be observed from Fig. 5 that the proposed EPLT scheme possesses better performance comparing with the other two algorithms under different NLOS errors. Furthermore, the performance obtained from the PLT scheme is degraded with the increase of the NLOS errors. As a result, the effectiveness of the EPLT algorithm is perceived.

V. Conclusion

In this paper, the enhanced predictive location tracking (EPLT) scheme is proposed. With the predictive information obtained from the Kalman filtering formulation, additional measurement inputs are exploited and the signal sources become available for location estimation and tracking of a mobile device. Moreover, the EPLT algorithm adjusts the locations of its virtual Base Stations based on the geometric dilution of precision (GDOP) criterion. Consistent location estimation and tracking accuracy can be acquired by adopting the EPLT scheme with different scenario.

References

[1] M. Nájar and J. Vidal, "Kalman Tracking for Mobile Location in NLOS Situations," in *IEEE International Symposium on Personal, Indoor and Mobile Radio Communications (PIMRC)*, Sep. 2003, pp. 2203–2207.

[2] C. L. Chen and K. F. Feng, "Hybrid Location Estimation and Tracking System for Mobile Devices," in *IEEE Vehicular Technology Conference (VTC)*, Jun. 2005, pp. 2648–2652.

[3] Y.-C. Lin, P.-H. Tseng, and K.-T. Feng, "A Predictive Location Tracking Algorithm for Mobile Devices with Deficient Signal Sources," in *IEEE Vehicular Technology Conference (VTC)*, Apr. 2007, pp. 859–863.

[4] C. Y. Lee, *Mobile Communications Engineering*. McGraw-Halls, 1993.

[5] J. Chaffee and J. Abel, "GDOP and the Cramer-Rao Bound," in *IEEE Position Location and Navigation System (PLANS) Conference*, Apr. 1994, pp. 663–668.